PERFORMANCE ANALYSIS OF A SELF-PROTECTION SYSTEM FOR VEHICLES IN CASE OF WUI FIRE ENTRAPMENT

Elsa Pastor[1,*], Juan Sebastià[2], Christian Mata[1], Alba Àgueda[1], Mario Miguel Valero[1], Eulàlia Planas[1]
[1] Centre for Technological Risk Studies (CERTEC), Department of Chemical Engineering, Universitat Politècnica de Catalunya · BarcelonaTech, Catalonia
[2] Wildfire Security S.L., Spain

ABSTRACT

Sheltering inside a civilian vehicle has proved to be a high risk strategy in case of wildfire entrapment. Survival is by no means guaranteed, especially in moderate to high-intensity wildfires. However, vehicles do offer a certain degree of fire protection, which can be reinforced by *ad-hoc* fire resistant technology. In this paper, we present the experimental performance analysis of a self-protection system that has been designed to protect people's life in case of fire entrapment. Similar to a firefighter fire shelter, the designed system can be quickly deployed covering the whole vehicle. In case of fire exposure, this fabric provides additional heat protection to the occupants and the vehicle itself. An experimental burning was designed in order to simulate real fire exposure conditions in case of vehicle entrapment in a rural road. An *ex-situ* 2-m high fuel bed composed of *Pinus halepensis* fine logging slash was arranged in a 13 m long x 6 m wide area. Fire was ignited at one end of the fuel bed and spread driven by an induced constant air flow (3 m/s midflame wind speed). 2.8 m away from the other fuel bed end, a car covered with the fire protection fabric was placed, parallel to the fire. Data analysis provided mean values of fire rate of spread (2 m/s), fireline intensity (1800 kW/m), flame height (6.5 m), flame tilt angle (30º), flame depth (2 m), flame temperature (800 ºC) and flame emissive power (47.5 kW/m^2). Maximum air temperatures inside the vehicle ranged around 41-42.5 ºC during a period between 20 min and 35 min after ignition. A thermocouple in contact with the internal side of the driver's window registered a maximum value of 47.3 ºC. These results evidenced the good performance of the fabric when protecting eventual vehicle occupants against thermal exposure from wildfires of moderate intensity.

INTRODUCTION

Forest fires affecting communities represent a rising problem throughout the world. As the climate warms, hot and dry seasons are lengthening and wildfires are behaving more often as real fire storms with huge intensities and large destructive potential. In addition, human pressure at the wildland-urban interface (WUI) is continuously growing with an increase of ignitions, structures and population density in areas with high forest fire risk. WUI fires pose major management challenges in terms of civil protection and fire mitigation. These fires often exceed firefighter's capacities, who have to respond simultaneously to wildfire suppression, community evacuation and structures protection, hence becoming self-protection a growing need.

Recent WUI fire events have involved fatal consequences for population. Fire incident analysis has revealed that many of the casualties correspond to people caught on the road, either on foot or in vehicles, trying to escape from the fire. For instance, in 2017, Portugal experienced the deadliest WUI fires in its history, with more than 110 deaths. Particularly, 58 of them died in or near their cars when the fire overtook several rural roads. Wildfire in Attica (July 2018, Greece) also killed 99 people, a fair amount of them burnt in houses and cars. Thousands of vehicles were trapped when fleeing from the fire heading to the coastline.

Sheltering inside a civilian vehicle has proved to be a high risk strategy in case of wildfire entrapment. Survival is by no means guaranteed, especially in moderate to high-intensity wildfires[1]. However, vehicles do offer a certain degree of fire protection, which can be reinforced by *ad-hoc* fire resistant technology.

There is limited literature available (no peer-reviewed papers, according to the authors' knowledge) about the safety of people becoming entrapped in vehicles. In Table 1 studies conducted to monitor and compare air toxics levels, temperature and radiation conditions inside fire shelters, firefighters' engines and civilian cars are presented. Based on these results and considering recommendations of fire researchers, Australasian Fire Authorities Council provided guidelines for people who do find themselves in cars during bushfires[1]. The following advices are examples of those included in the document: 1. The car should be parked, ideally, on a non-combustible surface and should be positioned towards the oncoming fire front; 2. Inside the car, windows and doors should be tightly shut, the car vents should be closed, the engine should be turned off, occupants need to get down as low as possible (below the window level), and water should be drunk if possible to avoid dehydration.

As shown in Table 1, Mangan (1998)[2] tested firefighting vehicles and fire shelters in open field burns that reached high intensity heat fluxes. In this work details about test procedures and methods were very complete, but tenable and survivable cabin conditions were not mentioned. On the contrary, in the work from Brown et al. (2003)[3] tenability and survivability conditions were comprehensively reviewed for air toxics. For instance, CO exposure criteria for tenability and survivability were 100 ppm and 1000 ppm, respectively. In the work from Knight et al. (2003)[4] survivable cabin conditions for temperature and radiation exposures were established as limiting values that should only be endured for less than a minute, i.e. 2 kW/m^2 of radiation direct to the person and 200 ºC of blast of hot air. Sargeant et al. (2007)[5] referred to Brown et al. (2003)[3] for air toxics tenable and survivable conditions, and survivable cabin conditions for temperature and radiation exposures were based on Knight et al. (2003)[4] work.

Maximum/minimum inside temperatures registered in the works from Sargeant et al. (2007)[5] and Mangan (1998)[2] were 312.4 ºC/38 ºC and 280 ºC/60 ºC, respectively. Maximum temperatures were registered in tests where the physical integrity of the vehicle was breached.

Table 1. Experimental studies performed to test fire shelters, firefighters engines and civilian cars performance against fire. NA: Not available.

Study	**Specimens**	**System for protecting the vehicle cabin**	**Inside measurements**	**Fire source (intensity)**	**Maximum Heat flux**
Sargeant et al. (2007)[5]	Used cars in operable conditions	-	Respirable particles, CO, HCL, HCN Temperature Total heat flux	LPG gas-fired grid (NA)	0.028–1.7 kW/m^2 (inside, below window)
Brown et al. (2003)[3]	Firefighting vehicles	Radiation shields or watersprays	Respirable particles, CO, HCl, formaldehyde, TVOC	LPG gas-fired grid (5-10 MW/m)	NA
Knight et al. (2003)[4]	Firefighting trucks	Radiation shields, watersprays	Temperature Radiant heat flux	LPG gas-fired grid (2.5-10 MW/m)	0.5-10 kW/m^2 (inside)
Mangan (1998)[2]	Firefighting vehicles and fire shelters	-	Particles, HCl, HCN, SO2, Benzene, toluene, CO Temperature Radiant heat flux	Grass, brush or timber fuel (NA)	70-150 kW/m^2 (outside)

Another approach for protecting firefighters in case of fire entrapment was invented in Australia, that is the so-called Burn Over Protection Unit[6]. *Folded into a cabinet on top of the water tanks at the rear of a fire pump truck, the hi-tech heat resistant "tent" drops down over three people in a matter of seconds, providing a temporary protective refuge while a fire front passes*[6]. This system was devised as an alternative from staying in the cab of the vehicle, where smoke and plastic fumes can accumulate.

In Portugal recent research efforts are being carried out to implement a fabric that can be used to protect firefighters sheltering in the cabins during burnover. According to the main researcher of the FIRE PROTECT project, thanks to this fabric maximum temperatures between 50 ºC and 60 ºC can be reached inside firefighters vehicles. Despite they mention that the canvas would be an option for protecting civilian cars, they consider that it would not be suited for protecting people staying inside their vehicles[7]. In fact, the threshold for pain regarding ambient temperature (46 ºC) is lower than the above-mentioned temperature range. Moreover, 50 ºC is also considered intolerable with dew-points greater than 25 ºC[8].

In this paper, we present the experimental performance analysis of a self-protection system that has been designed to protect people's life in case of fire entrapment. Similar to a firefighter fire shelter, the designed system consists of 1 mm depth 3-layer fabric (aluminium, intumescent material and ceramic foils). It is lightweight (608 g/m^2), fire resistant and can be quickly deployed covering the whole vehicle. In case of fire exposure, this fabric provides additional heat protection to the occupants and to the vehicle itself.

MATERIALS AND METHODS

Experimental layout

An experimental burning was designed to simulate real fire exposure conditions in case of vehicle entrapment in a rural road. An *ex-situ* 2-m high fuel bed of fine *Pinus halepensis* logging slash was arranged in a 13 m long x 6 m wide flat area at the Wildfire Security SL outdoor testing facilities (Puçol, Spain). The fuel bed had 3 zones (A, B, C), being two of them continuous (A and B). Between these zones and zone C, there was a 6.1-m wide fuel-cleared space simulating a road, in which a car (Renault Mégane Sedan) was located (Figure 1).

Fuel load and fuel continuity was qualitatively assessed. Fuel in zone A was mainly horizontally oriented whereas fuel in zone B and C had vertical orientation. As a reference, the fuel bed could be treated as a logging slash fuel model in zone A and as a high density sapling stand fuel model in zones B and C. However, no specific assignation could be done to any particular standard fuel model (i.e. those from [9] or [10]) since no quantitative fuel sampling was performed to measure fuel parameters.

Data acquisition

During the burning, different sensors were deployed to characterize environmental variables, fire behaviour parameters and the efficiency of the fire-protection fabric. Regarding environmental variables, ambient temperature, relative humidity and 2.5 m wind speed and direction were monitored at 30 m distance from the SE side of the fuel bed (Kestrel 4500, Kestrelmeters, 1 datum every 30 seconds). Fuel samples (<6 mm, 0.6 cm - 2.5 cm) were randomly collected 10 minutes before ignition and oven-dried in the laboratory (90ºC, 24h) for moisture content analysis. An airflow parallel to the fuel bed orientation was induced one minute before ignition using a fan located at 5 m from the southern corner of the fuel bed. Induced wind speed was monitored at 1.5 m with a portable anemometer (Kestrel 4500, Kestrelmeters) by the time of ignition. Fire behaviour was monitored by infrared (IR) recording systems (Table 2) and video cameras (one of them mounted on a surveillance drone from the València Fire Emergency Agency). The efficiency of the fire protection fabric was deduced by analysing temperature data acquired inside and outside the vehicle and between the fabric and the vehicle, during the fire progression. K-type thermocouples (0.5 mm and 1 mm diameter) were used connected to data HOBO® Onset U12-014 data loggers (1 datum per second).

Table 3 shows the thermocouples numbering system and their location. Figure 2 depicts several images of the experimental methodology.

a)

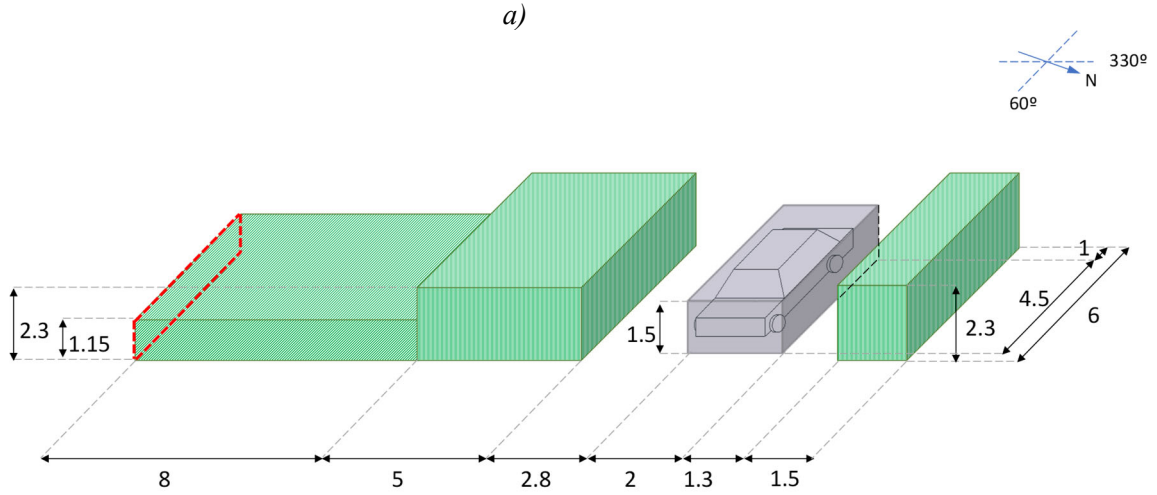

b)

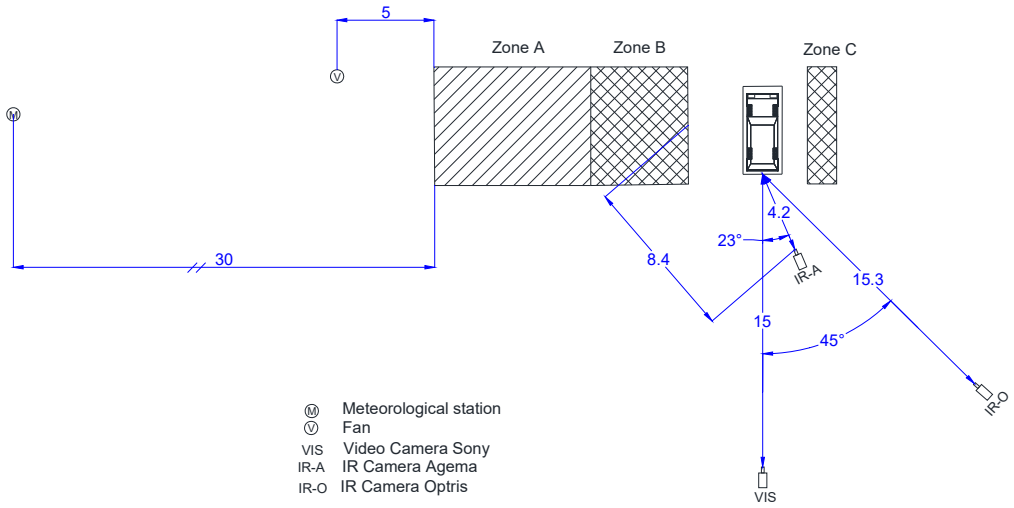

Figure 1. a) 3D sketch of the experimental layout. Doted red line shows the ignition zone (a 6-m ignition line was performed by professional fire-fighters using drip-torches in less than one minute); b) Plan view of equipment location (distances in m).

Table 2. Infrared cameras specifications

Equipment	AGEMA Thermovision 570 – Pro (FSI FLIR Systems)	Thermal Imager Optris Pi 640 (OPTRIS)
Detector	FPA (Focal Plane Array), non-refrigerated microbolometer	FPA (Focal Plane Array), non-refrigerated microbolometer
Brightness temperature range (ºC)	-20 - 1500	-20 - 900
Thermal sensitivity (ºC)	0.15	0.075
Field of view (º)	24º x 18º	60°×45°
Spectral range (µm)	7.5 - 13	7.5 - 13
Image size	320 x 240 pixel	640 x 480 pixel
Operation mode	Discontinuous	Continuous recording (32 fps)

Table 3. Thermocouples location

ID Zone	Description	Thermocouples numbering
ZI	Vehicle inside. Thermocouples placed at head's height (seated passengers)	Driver space: Ti 3 Copilot space: Ti 5 and Ti 6 Backseat (rear driver) space: Ti 1 Backseat (rear copilot) space: Ti 4, Ti 7 and Ti 2. Driver window: Ti w
ZE	Vehicle outside: Thermocouples placed close to the external surface of the fire-protection fabric (fire exposure from Zone B)	Motor zone: Te 1 Boot zone: Te 2 Driver door zone: Te 3 and Te 4
ZM	Intermediate zone: Thermocouples placed between the internal surface of the fire-protection fabric and the external casing of the vehicle (fire exposure from Zone B)	Motor zone: Tm 1 Rear door zone: Tm 2 Driver door zone: Tm 3

a) *b)*

c) *d)*

Figure 2. Experimental design; a) side view and b) view from above of the experimental site; c) thermocouples located at the co-pilot seat at head's height; d) thermocouple located at the internal side of driver's window

RESULTS AND DISCUSSION

Environmental conditions and fuel moisture content

The overall period under study comprised 40 minutes, from 11:40:00 to 12:20:00, being ignition time at 11:53:25. Mean ambient temperature recorded during the experiment was 27.6 ºC (s.d. 1.18 ºC) and mean relative humidity was 59.2 % (s.d. 4.32 %). The prevailing south-easterly wind had mean speed of 3 m/s during the fire progression (s.d. 1.33 m/s). The induced air flow had a mean spead of 3 m/s at 1.5 m. Fuel moisture content (calculated at dry bases) was 26.7 % (s.d. 8.4 %) for the lowest diameter class (< 6 mm) and 26.2 % (s.d. 5.7 %) for the highest (0.6 cm to 2.5 cm).

Fire progression

Fire spread was monitored as it progressed through zones A and B of the fuel bed. Drone imagery acquired from a nadir perspective was used to delineate fire progression isochrones every 30 seconds (Figure 3, a)). Isochrones were annotated manually and subsequently processed to compute fire rate of spread (ROS). Fire spread direction was assumed perpendicular to the fire perimeter, and ROS was estimated at every isochrone point as the distance travelled by fire in that direction divided by the time elapsed between consecutive isochrones. These point values were interpolated linearly to create a 2D ROS field (Figure 3, b)). ROS values obtained through this methodology are therefore spatially explicit and averaged over 30 seconds time intervals.

Measured fire spread direction was clearly aligned with induced wind, creating a pseudo-elliptical front (see isochrones #3 and #4) with maximum ROS values of 6 m/min. Average perimeter ROS varied with time between 1.3 and 2.7 m/min. In addition to surface spread, short-range spotting was observed (Figure 4).

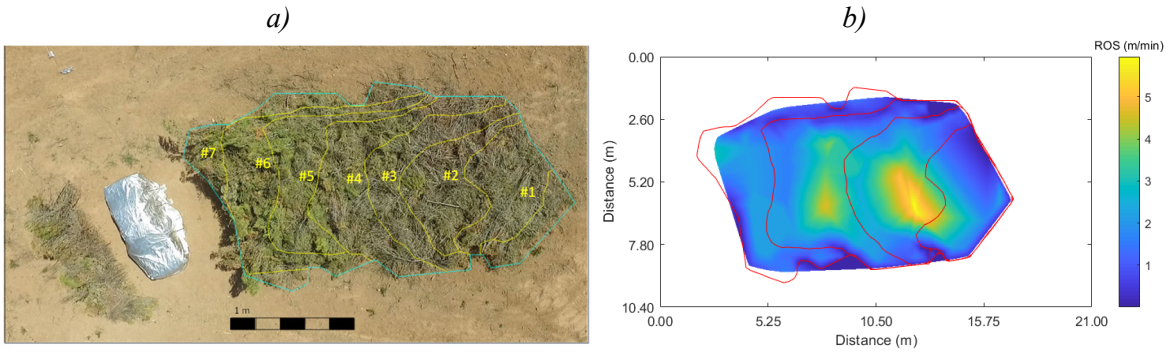

Figure 3. a) Fire progression isochrones computed every 30 seconds; and b) resulting rate of spread (right). ROS field was interpolated linearly from point estimations obtained along every isochrone.

Figure 4. Aerial snapshot acquired 2min 08sec after ignition, showing short-range spotting.

Figure 5. Video snapshot acquired 4min 03sec after ignition, showing highest car exposure to flames.

Fire reached the fuel bed end approximately 3 minutes and 30 seconds after ignition (isochrone #7), where flaming persisted for about 7.5 minutes. Maximum car exposure to flames occurred around 4 minutes after ignition (Figure 5). No direct contact between flame and fabric was observed.

Finally, fuel zone C was ignited by fire brands 5 minutes after the start of the experiment, burning actively until all fuel was consumed.

Fire line intensity

Byram's fire line intensity[11,12] was estimated according to previously computed ROS (mean values of 2.1 m/min and 1.6 m/min, for Zone A and B, respectively) and following educated assumptions on the amount of fuel consumed by the flames. Fine fuel was assumed to be consumed completely during fire front residence time. Fine fuel loads were estimated to be 27.2 t/ha for zone A and 30 t/ha for zone B, according to fuel models described in [13,14] for *Pinus halepensis* sapling stands. Measured fuel moisture content (26.7 %) and literature values for *Pinus halepensis* high calorific value (20700 kJ/kg[15]) yielded average fire line intensities of 1500-1800 kW/m, with intensity peaks of up to 5100-5600 kW/m.

Flame geometry

Mean flame dimensions were computed by using image segmentation techniques[16] (Figure 6). The period analysed covered the last 30 s of the fire progression and the first minute of continuous flaming at the interface between the Zone B and the fuel-cleared space. This time interval is representative of the highest fire exposure experienced by the protected vehicle. Flame geometry could hence be described by a flame height of around 6.5 m (mean value 6.38 m, s.d. 1.22 m), a tilt angle of 30º (mean value 27.87º, s.d. 4.6º) and a flame depth of around 2 m (mean value 1.79 m, s.d. 2.02 m).

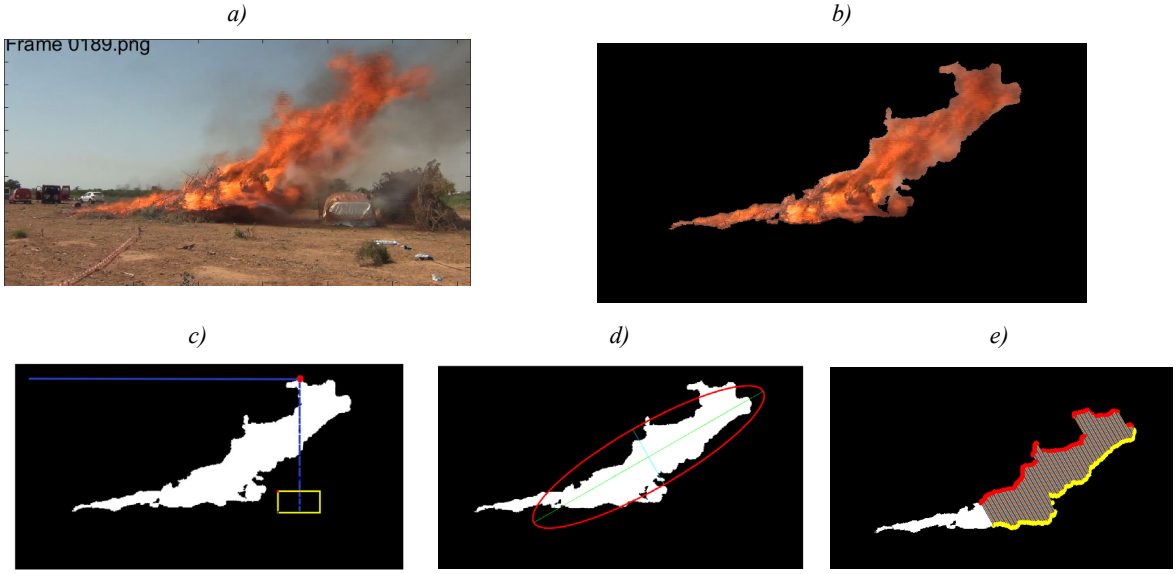

Figure 6. Segmentation process and flame geometry analysis. a) Visual image recorded by a video camera; b) flame segmentation; c) flame height analysis: the yellow line shows the vehicle contour, the blue dotted line goes from the basis of the vehicle to the highest flame point; d) flame tilt analysis; e) flame depth analysis

Flame temperatures and emissive power

Flame temperatures and emissive power were estimated for the period of highest fire exposure by analysing IR imagery with Thermacam Researcher Pro 2.10 Software (Figure 7). Considering an emissivity of 0.7 for a 2 m-depth flame[17], and a distance of 8.4 m from the sensor to the flames, mean and maximum temperatures were obtained around 800 ºC (mean value of 772ºC, s.d. 47.6 ºC) and 1200

ºC (mean value of 1173 ºC, s.d. 52.3 ºC) respectively. According to Stefan-Boltzmann law, mean flame emissive power was around 47.5 kW/m^2 with maximum values of 75.5 kW/m^2.

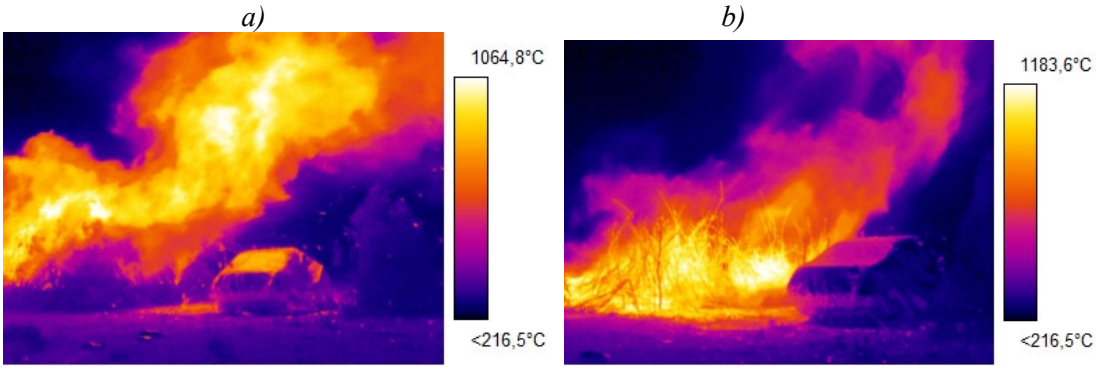

Figure 7. IR images of the period of highest fire exposure; a) beginning of the period; b) end of the period

Temperatures

Temperatures outside the fabric

Figure 8 shows temperatures registered by the four thermocouples located outside the fabric. The effect of the heat emitted by the fire starts being noticed around 1:50 min after ignition. Maximum temperature values are observed between minutes 03:51 (maximum value of 137.6 °C registered by thermocouple Te 4) and 05:02 (maximum value of 111.4 °C registered by thermocouple Te 2). The highest value recorded during this period is 201.5 °C at minute 04:06, corresponding to thermocouple Te 1. This period coincides with the continuous presence of flames in the interface between the Zone B and the fuel-cleared space, where practically the whole width of the fuel is burning. These temperature values show that –at the location of the sensors– there was no direct contact of the flames with the thermocouples (the minimum temperature that can be expected for the presence of flames is about 350 °C[18]. After this period, there is a general temperature decreasing trend for the four thermocouples. This global decrease is, however fluctuating, i.e. peaks and valleys are observed all along the temperature evolution. These fire dynamics are consistent with the pulsating behaviour typically observed in forest fires[19,20], due to intermittent fresh air indraft from the unburned fuel, producing a cooling effect. During the last minute (around 33 minutes after ignition), temperatures fluctuate between 31.7 °C and 52.5 °C (mean value of 43 °C), being mean ambient temperature 31 ºC at that moment.

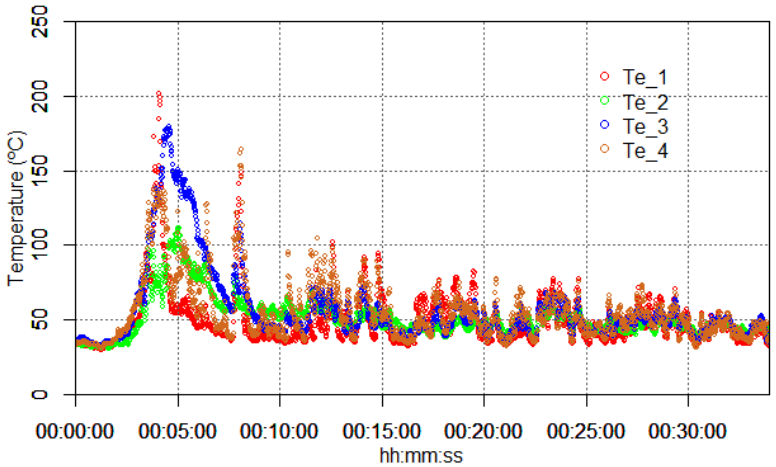

Figure 8. Temperature versus time evolution for the four thermocouples located outside the fabric.

Initial time on the graph coincides with the ignition time.

Temperatures in-between the fabric and the vehicle

The effectiveness of the fabric as thermal insulator can be seen in Figure 9. The general trend is similar to the one reported in the previous section, although in this case the evolution is smoother and a few seconds delayed. Temperatures start to increase significantly 2.5 minutes after ignition (in the case of outside temperatures this increase was 40 s earlier) and reach a maximum between instant 04:24 (thermocouple Tm 1 registers a maximum of 58.7 °C) and instant 4:47 (thermocouple Tm 2 reaches 68.5 °C). In this period, the maximum temperature value recorded is 74.4 °C (by thermocouple Tm 3, 04:43 min after ignition), with a delay of 37 s with respect to the maximum value recorded outside the fabric, and a value 63 % lower. A similar fluctuating decreasing behaviour is also observed. In this case though, the pulse of the fluctuation is lower, both with respect to the frequency and to the temperature range. During the last minute, temperatures oscillate between 41.3 °C and 45 °C, with a mean value of 43.1 °C, almost equal to the outside temperature at the fabric registered during this period.

For a better comparison between outside fabric temperatures and the temperatures in-between the fabric and the vehicle, Figure 10 shows the temperature evolution for thermocouples Te 1 and Tm 3. Both thermocouples recorded the highest temperature values of their zone (ZE for Te 1 and ZM for Tm).

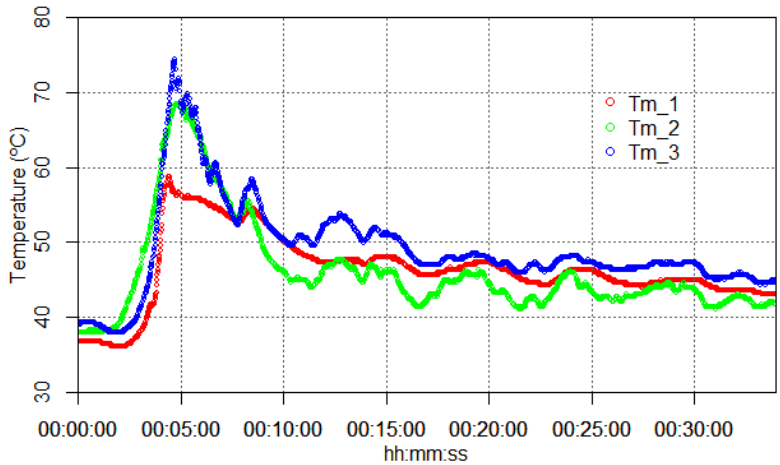

Figure 9. Temperature vs time evolution for the three thermocouples located in-between the canvas and the vehicle. Initial time on the graph coincides with the ignition time.

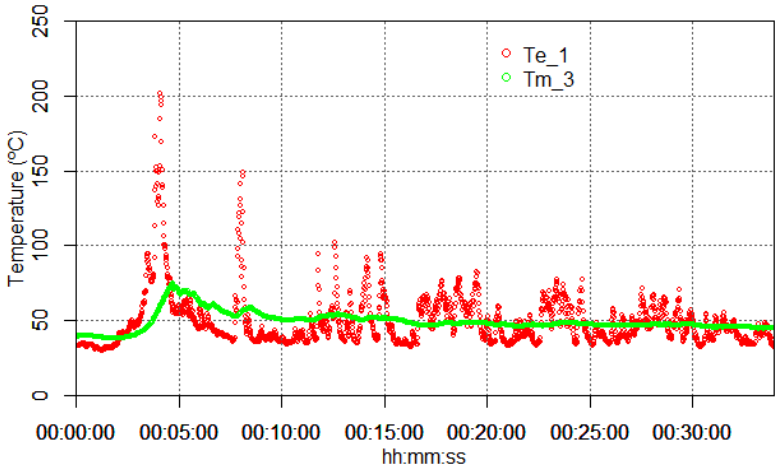

Figure 10. Temperature vs time evolution for thermocouples Te 1 (located outside the canvas) and Tm 3 (located in-between the canvas and the vehicle).

Temperatures inside the vehicle

Temperature values registered by the thermocouples located inside the vehicle are shown in Figure 11. A significant difference can be observed between the temperature evolution of the thermocouple located in contact with the inside surface of the driver's window and the temperature evolution of all the other thermocouples, located at head's height on the front and back seat positions. Temperatures registered by the thermocouples located at the head's height increase monotonically five minutes after ignition. Maximum values are achieved 20 to 35 minutes after ignition. Table 4 shows the maximum values recorded which are around 41 – 42.5 °C. There are no significant differences between thermocouples due to their location. 35 minutes after ignition, a clear temperature decrease is observed. During the last minute, temperatures are very stable in all thermocouples and very similar to each other, with an average value of 39.2 °C (s.d. 0.25 °C). Regarding the thermocouple located in contact with the driver's window, it registers a temperature increase 03:30 minutes after ignition, reaching a maximum value of 47.3 °C 08:55 minutes after ignition. From then on, it experiences a gentle descent until minute 33, after which the decrease becomes more pronounced.

Figure 12 shows the temperature evolution for thermocouples Tm 3 and Ti 6, for a better comparison between temperatures recorded in-between the fabric and the vehicle and the temperatures recorded inside the vehicle, respectively. Both thermocouples recorded the highest temperature values of their zone (ZM for Tm 3 and ZI for Ti 6).

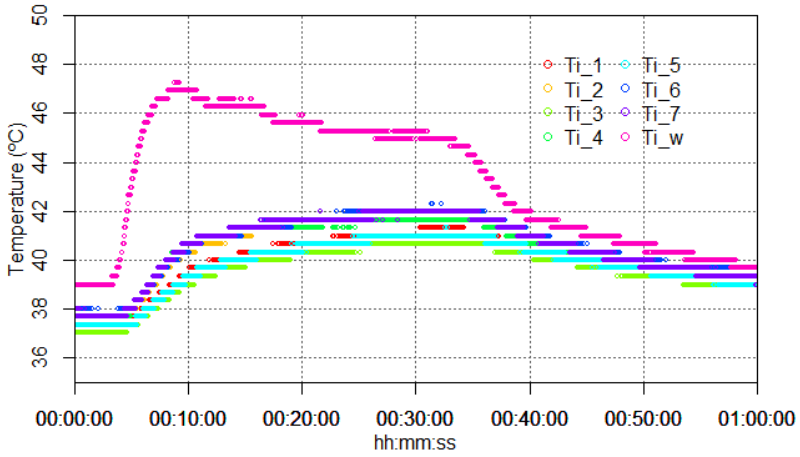

Figure 11. Temperature vs time evolution for the six thermocouples located inside the vehicle. Initial time on the graph coincides with the ignition time.

Table 4. Maximum temperature values recorded by the thermocouples located inside the vehicle.

Thermocouple	Time (min:s)	Temperature (ºC)
Ti 1	30:26	41.31
Ti 2	27:04	41.97
Ti 3	30:34	40.98
Ti 4	31:30	41.97
Ti 5	32:48	41.31
Ti 6	31:25	42.30
Ti 7	21:32	41.97
Ti w	08:55	47.25

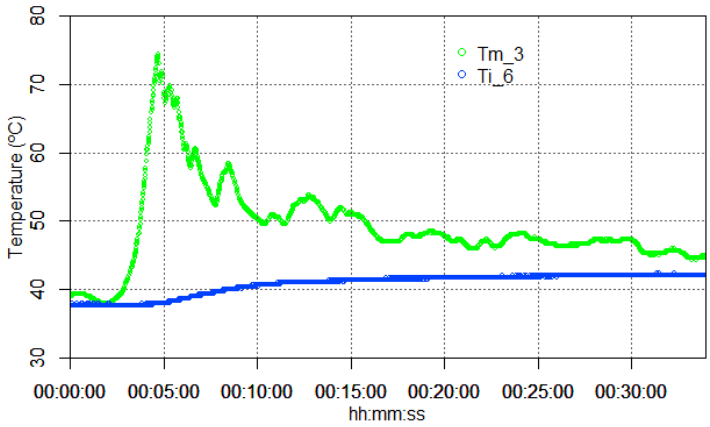

Figure 12. Temperature vs time evolution for thermocouples Tm 3 (located in-between the canvas and the vehicle) and Ti 6 (located inside the vehicle).

Under the conditions of this experiment, temperature values reached inside the vehicle do not pose any risk to people. The limit for pain regarding ambient temperature is around 46 °C[8]. As reported, these values are never reached inside the vehicle. On the other hand, the limit for experiencing pain by heat conduction is set at 60 °C[8]. Temperatures on the window surface do not reach this threshold, so that contact with the glass would not cause damage to the occupants either.

CONCLUSIONS

- The experimental set-up has allowed emulating fire exposures typical of an incipient surface fire of moderate intensity (mean rate of spread of 2 m/min and average fire intensity below 1800 kW/m).
- The methods used have allowed to characterize the fire in the best possible way, given the current state of technology. Still, it is worth considering the error associated with experimentation and uncertainty of the calculation methods. Therefore, the fire behaviour values reported should be taken as reasonable estimates.
- In the conditions of this experiment, the effects on people due to the increase in temperature would not be significant in adults in good health who were located inside the protected vehicle. However, this does not necessarily guarantee their survival since the risk of intoxication due to inhalation of combustion gases or the lack of oxygen inside the vehicle, would also need to be evaluated.
- The experiment proves that the fabric performs well to protect people from an eventual temperature increase inside the vehicle, provided that the conditions to which the vehicle has been exposed, both in terms of radiant heat flux and exposure time, are similar or less intense than those tested in this experiment.
- To analyse the response of the fire shelter fabric to more severe conditions (i.e. higher radiant heat fluxes and longer duration), it would be necessary to perform new tests with an experimental set-up allowing to replicate more intense wildfire exposure.

REFERENCES

[1] Australasian Fire Authorities Council (AFAC) (2008). Guidelines for people in cars during bushfires. Available at: https://www.chillipreppers.com.au/uploads/5/9/5/1/5951747/fire-guidlines-people-in-vehicles.pdf

[2] Mangan, R. (1998). Surviving fire entrapments: comparing conditions inside vehicles and fire shelters. Tech. Rep. 9751-2817-MTDC. Missoula, MT: US Department of Agriculture, Forest Service, Missoula Technology and Development Centre.

[3] Brown, S.K., Cheng, M., Mahoney, K.J., Leonard, J., Nichols, D., Canderle, A., Knight, I. (2003). Air toxics factors and criteria for crew survivability/tenability in vehicle burnover. 21st Annual conference of the Australian Institute of Occupational Hygienists, "Improving occupational hygiene in small business", Dec. 6-10, 2003, Adelaide, Australia
[4] Knight et al. (2003). Thermal factors for human survival in fire tanker burn-overs. Presented to 3rd International Wildland Fire Conference, 3-6 October, Sydney, Australia
[5] Sargeant, A., Brown, S., Leonard, J., Blanchi, R. (2007). Civilian passenger vehicle burnover experimentation. Paper presented to 2007 Joint AFAC/Bushfire CRC Conference
[6] NEWS (2015) https://www.abc.net.au/news/2015-06-28/wa-volunteer-firefighter-develops-fire-shield/6578956
[7] eldiario.es (2019) https://www.eldiario.es/sociedad/Inventan-sintetica-salvar-incendios-forestales_0_881911998.html
[8] Bradshaw, V. (2006). The building environment: active and passive control systems. John Wiley and Sons.
[9] Rothermel, R.C., 1972. A mathematical model for predicting fire spread in wildland fuels. USDA Forest Service, Intermountain Forest & Range Experiment Station. Res. Pap. INT-115.
[10] Scott and Burgan (2005). Standard fire behaviour fuel models: a comprehensive set for use with Rothermel's surface fire spread model. USDA Forest Service, Rocky Mountain Research Station. Gen Tech Rep, RMRS-GTR-153.
[11] Byram GM. (1959). Combustion of forest fuels. In: Forest fire control and use. Davis KP, McGraw-hill Book Co, New York.
[12] Alexander, M.E. (1980). Calculating and interpreting forest fire intensities. Canadian Journal of Botany, 60, 349-357.
[13] Domènech, R. (2011). Efectivitat dels tractaments d'aclarida en la reducció del risc de propagació d'incendis en regenerats de pi blanc. Tesi Doctoral. Universitat Politècnica de Catalunya. 235 pp.
[14] Domènech, R., Pastor, E., Àgueda, A., Sans, A., Navascués, P., Planas, E. (2013). Modelos de combustible para caracterizar el comportamiento de los incendios en regenerados clareados de pino carrasco. Montes, 115, 22-29.
[15] Guijarro, M., Hernando, C., Díez, C., Martínez, E., Madrigal, J., Lampin, C., Blanc, L…Fonturbel, M. (2002). Flammability of some fuel beds common in the South-European ecosystems. En: D.X. Viegas (Ed.), Forest Fire Research and Wildland Fire Safety, Millpress, Rotherdam, 1-9.
[16] Mata, C., Pastor, E., Rengel, B., Valero, M., Planas, E., Palacios, A. and Casal, J. (2018). Infrared Imaging Software for Jet Fire Analysis. The Italian Association of Chemical Engineering (AIDIC), ISBN 978-88-95608-64-8, Vol. 67.
[17] Àgueda, A., Pastor, E., Pérez, Y., Planas, E. (2010). Experimental study of the emissivity of flames resulting from the combustion of forest fuels. International Journal of Thermal Sciences, 49(3), 1-12.
[18] Babrauskas, V. (2006). Temperatures in flames and fires. Fire Science and Technology Inc. San Diego, CA.
[19] Frankman, D., Webb, B. W., Butler, B. W., Jimenez, D., Forthofer, J. M., Sopko, P., Ottmar, R. D. (2013). Measurements of convective and radiative heating in wildland fires. International Journal of Wildland Fire, 22(2), 157–167.
[20] Tang, W., Gorham, D. J., Finney, M. A., Mcallister, S., Cohen, J., Forthofer, J., & Gollner, M. J. (2017). An experimental study on the intermittent extension of flames in wind-driven fires. Fire Safety Journal, 91, 742–748.